One-Way Electromagnetic Mode Guided by the Mechanism of Total Internal Reflection

Linfang Shen, Jie Xu, Yun You, Kai Yuan, and Xiaohua Deng

***Abstract*— One-way electromagnetic mode that is guided by the mechanism of total internal reflection (TIR) can be realized in terahertz regime. In the optical system consisting of a dielectric layer sandwiched between magnetized semiconductor and metal, the one-way TIR mode can be immune to backscattering at imperfections. This mode possesses a broad band when high-order TIR modes are suppressed in the relevant semiconductor bandgap. Furthermore, it is shown that compared with one-way surface magnetoplasmons, the one-way TIR mode can more effectively match with the fundamental mode of conventional optical waveguide.**

***Index Terms*— Nonreciprocity, waveguide, one-way propagation, terahertz.**

I. Introduction

ONE-WAY electromagnetic (EM) modes are such modes that they are allowed to propagate in only one direction, and because of the absence of a back-propagating mode in the system, they are immune to backscattering at imperfections. One-way EM modes were first proposed as analogues of quantum Hall edge states in photonic crystals (PhCs) [1], [2]. These one-way modes can be sustained by the edges of certain two-dimensional (2D) PhCs made of magnetic-optical (MO) materials [1]–[5], whose time-reversal symmetry is broken by applied dc magnetic field. Other type of one-way surface wave, i.e., one-way surface magnetoplasmon (SMP) [6], was also proposed later [7], [8]. One-way SMPs can be supported by bulk plasmonic materials in optical [7] or terahertz regimes [9], [10]. In microwave domain, one-way SMPs can be supported by yttrium-iron-garnet (YIG) materials [11]. Recently, we reported a one-way EM mode which is not surface wave in the microwave regime [12]. Such one-way mode is guided by the mechanism of total internal reflection (TIR) in the system consisting of a dielectric layer sandwiched between magnetized YIG and metal.

It is interesting if one-way TIR modes can be realized by using plasmonic materials in the terahertz or optical regimes. Plasmonic materials, which are characterized by Drude model, have dispersion properties quite different from those of YIG, especially when they are magnetized. For example, the first zone of bulk modes does not have any low-frequency cut-off in YIG, whereas it has one in semiconductors, which are plasmonic materials used in terahertz regime. Moreover, SMPs in YIG can exhibit resonance in only one direction, whereas SMPs in semiconductors exhibit resonances in both (forward and backward) directions at different asymptotic frequencies [10], [12]. Therefore, the existence of one-way TIR mode in the terahertz or optical regimes is still a problem to study. At higher frequencies, one-way TIR modes are more attractive, as one-way waveguides of such type should be well compatible with conventional optical waveguides there, which are guiding waves based on the TIR mechanism [13]. In this letter, we will show that by using semiconductor, one-way TIR mode can be realized in terahertz regime. Moreover, we will numerically demonstrate that compared with one-way SMP, one-way TIR mode can more effectively match with the fundamental mode of conventional optical waveguide.

II. Theoretical Analysis and Numerical Simulation

We consider a guiding structure consisting of a silicon (Si) layer sandwiched between semiconductor and metal, as illustrated in the inset of Fig. 1(a). The Si layer has a relative permittivity of $\varepsilon_r = 11.68$, and its thickness is denoted by d. The metal is approximated as perfect electric conductor (PEC), which is valid for terahertz regime. In order to break the time-reversal symmetry of the guiding system, a dc magnetic field is applied in the y direction, thus the semiconductor becomes gyroelectrically anisotropic, whose (relative) permittivity has the form

$$\overleftrightarrow{\varepsilon}_s = \begin{bmatrix} \varepsilon_1 & 0 & -i\varepsilon_2 \\ 0 & \varepsilon_3 & 0 \\ i\varepsilon_2 & 0 & \varepsilon_1 \end{bmatrix}. \tag{1}$$

The tensor elements in Eq. (1) are $\varepsilon_1 = \varepsilon_\infty[1-\omega_p^2/(\omega^2-\omega_c^2)]$, $\varepsilon_2 = \varepsilon_\infty\omega_c\omega_p^2/[\omega(\omega^2-\omega_c^2)]$, and $\varepsilon_3 = \varepsilon_\infty(1-\omega_p^2/\omega^2)$, where ω is the angular frequency, ω_p is the (effective) plasma frequency of the semiconductor, $\omega_c = eB_0/m^*$ (where e and m^* are, respectively, the charge and effective mass of the electron) is the electron cyclotron frequency, and ε_∞ is the high-frequency (relative) permittivity. In this letter, the semiconductor is assumed to be InSb with $\varepsilon_\infty = 15.7$ and $\omega_p \approx 4\pi \times 10^{12}$ rad/s (correspondingly the plasma frequency $f_p = 2$ THz) [14]; the electron cyclotron frequency is set to be $\omega_c = \omega_p$ (corresponding to $B_0 = 1$ T).

Manuscript received January 13, 2017; revised July 9, 2017; accepted November 13, 2017. Date of publication November 21, 2017; date of current version January 3, 2018. This work was supported in part by the National Natural Science Foundation of China under Grant 61372005 and in part by the National Natural Science Foundation of China through a key project under Grant 41331070. *(Corresponding author: Kai Yuan.)*

The authors are with the Institute of Space Science and Technology, Nanchang University, Nanchang 330031, China (e-mail: y_k_phy@163.com).

Color versions of one or more of the figures in this letter are available online at http://ieeexplore.ieee.org.

Digital Object Identifier 10.1109/LPT.2017.2776106

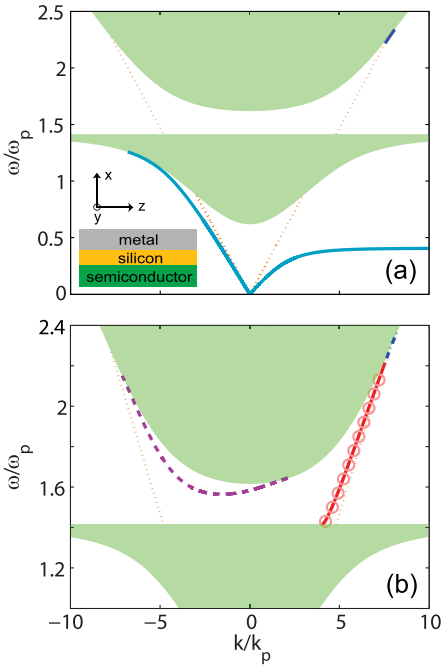

Fig. 1. (Color online) (a) Dispersion curves of SMPs. The inset is a schematic of the guiding system. (b) Dispersion curves of one-way (solid) and high-order (dashed) TIR modes in the system. The dispersion relation for the one-way TIR mode (solid line) in the PEC approximation agrees well with that (open circles) in the realistic case with Cu. The dash-dotted line represents the SMP band at higher frequencies in (a). In both (a) and (b), dotted lines represent the light lines in Si, and shaded areas are the bulk-mode zones in the semiconductor. The parameters of the system are as follows: $\varepsilon_\infty = 15.7$, $\omega_c = \omega_p$; $\varepsilon_r = 11.68$, $d = 0.06\lambda_p$.

It is known that the system under consideration can sustain SMPs, whose dispersion relation is written as [10]

$$\alpha - \frac{\varepsilon_2}{\varepsilon_1}k + \frac{\varepsilon_\mathrm{v}}{\varepsilon_r}\alpha_d \tanh(\alpha_d d) = 0, \tag{2}$$

where k is the propagation constant, $\alpha_d = \sqrt{k^2 - \varepsilon_r k_0^2}$ with $k_0 = \omega/c$ (where c is the light speed in vacuum), and $\alpha = \sqrt{k^2 - \varepsilon_\mathrm{v} k_0^2}$ with $\varepsilon_\mathrm{v} = \varepsilon_1 - \varepsilon_2^2/\varepsilon_1$ being the Voigt permittivity. Figure 1(a) shows the dispersion relation for SMPs, where d is taken to be $0.06\lambda_p$ ($\lambda_p = c/f_p$). Due to the nonreciprocity, the dispersion curves for SMPs with $k > 0$ and $k < 0$ (below the first zone of bulk modes in InSb) are asymmetric, and there exists a frequency interval, in which SMPs are only allowed to propagate backward. Moreover, beside the second zone of bulk modes in InSb, there exists another SMP band, at which SMPs only propagate forward.

The SMP band at higher frequencies is very narrow but particularly of our interest, as it intersects light line in Si. It seems possible that this dispersion band could be extended into the light cone in Si. This means that there probably exists one-way mode guided by the TIR mechanism. Letting $\alpha = ip$ (where p is real-valued), it follows from Eq. (2) that

$$\alpha - \frac{\varepsilon_2}{\varepsilon_1}k - \frac{\varepsilon_\mathrm{v}}{\varepsilon_r}p \tan(pd) = 0, \tag{3}$$

which is the dispersion relation for TIR modes in the system. Our numerical analysis shows that a TIR mode, whose band links the narrow SMP band at the light line, really exists, as shown in Fig. 1(b). This TIR band (solid line) is terminated from below at $\omega_{r,b} = \sqrt{\omega_c^2 + \omega_p^2}$, and the whole band has a positive slope, meaning that the mode only propagates forward. To examine the PEC approximation for metal in the above analysis, we also calculated the one-way TIR mode for a realistic case, where the metal was copper (Cu) described by a Drude model [15]. The obtained results are also plotted as open circles in Fig. 1(b), and they agree well with those for the PEC case. But in the case with Cu, the propagation length (L_p) of the one-way TIR mode becomes finite, e.g., $L_p = 585$ μm at $f = 3.2$ THz (i.e., $\omega = 1.6\omega_p$). For the considered system, there also exists another TIR mode (dashed line) with a higher cutoff frequency, as shown in Fig. 1(b). This high-order mode can propagate in both directions, like guiding modes in conventional optical waveguide. But in the semiconductor bandgap, there still exists a frequency region from $1.41\omega_p$ to $1.56\omega_p$, where no backward-propagating mode exists, and we refer to it as the complete one-way propagation (COWP) region. In the COWP region, the one-way TIR mode is immune to backscattering.

It is desired that by reducing the guiding-layer thickness, the high-order TIR mode may be shifted out of the semiconductor bandgap, thus broad COWP band is attained for the one-way TIR mode. Due to the nonreciprocity, the dispersion band for the high-order TIR mode is asymmetric with respect to k, but the cutoff deviates only a little from $k = 0$. At $k = 0$, we have from Eq. (3) that $1 + \sqrt{-\varepsilon_\mathrm{v}/\varepsilon_r}\tan(\sqrt{\varepsilon_r}k_0 d) = 0$. In the semiconductor gap, $\varepsilon_\mathrm{v} < 0$, hence the high-order mode must vanish if $\sqrt{\varepsilon_r}k_0 d \le \pi/2$, where $k_0 = \omega_{cf,b}/c$ with $\omega_{cf,b} = \sqrt{\omega_p^2 + \omega_c^2/4} + \omega_c/2$, which is the upper limit of the (second) semiconductor bandgap. Thus, we obtain a conservative estimation of the critical d value for achieving broad COWP band

$$d_c = \frac{\lambda_p}{2\sqrt{\varepsilon_r}\left(\sqrt{\bar{\omega}_c^2 + 4} + \bar{\omega}_c\right)}, \tag{4}$$

where $\bar{\omega}_c = \omega_c/\omega_p$. For the considered system with $\bar{\omega}_c = 1$, it is found that $d_c = 0.045\lambda_p = 6.8$ μm. Figure 2(a) shows the dispersion diagram for the case of $d = 6.8$ μm. As expected, the COWP band for the TIR mode covers the whole semiconductor bandgap $[\omega_{r,b}, \omega_{cf,b}]$. This COWP range is preserved when d decreases from d_c. On the other hand, our numerical analysis shows that when d grows from d_c, the cut-off point of the high-order mode lowers, and consequently, the COWP range is compressed downward. When $d = 14.4$ μm, the high-order mode begins to touch the lower limit of the semiconductor bandgap. In such a case, the COWP region completely vanishes for the one-way TIR mode, as shown in Fig. 2(b)

To verify the properties of TIR modes in the guiding system, we performed the simulation of wave transmission in it with the finite-element method. Two cases of $d = 6.8$ and 14.4 μm are analyzed. In the simulation, a magnetic current line source, which is located at the center of the Si layer, is used to excite guiding modes, and the frequency is $f = 3$ THz (i.e., $\omega = 1.5\omega_p$). The simulated magnetic field amplitudes

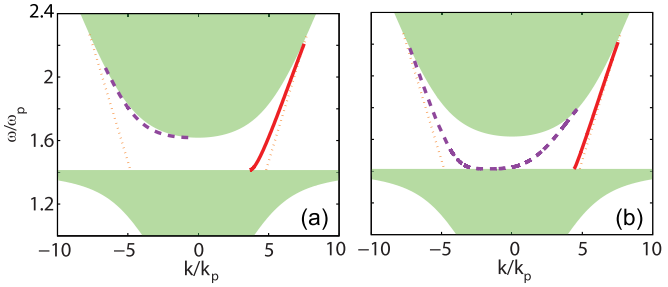

Fig. 2. (Color online) Dispersion curves of one-way (solid) and high-order (dashed) TIR modes. (a) $d = 6.8\ \mu$m, (b) $d = 14.4\ \mu$m. The other parameters are the same as in Fig. 1.

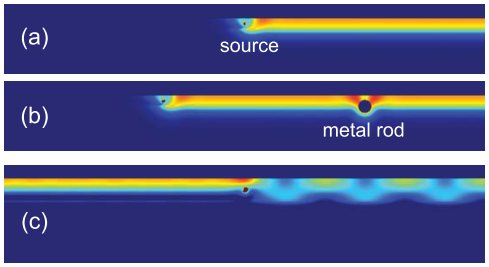

Fig. 3. (Color online) Simulated magnetic field amplitudes. (a) Uniform waveguide with $d = 6.8\ \mu$m, (b) the same waveguide as in (a) but with an obstacle, and (c) uniform waveguide with $d = 14.4\ \mu$m. The obstacle in (b) is a metal rod with the radius $r_o = 4\ \mu$m. The frequency is 3 THz for all cases. The other parameters are the same as in Fig. 1.

for $d = 6.8\ \mu$m are plotted in Fig. 3(a). As expected, the excited waves only travel forward. Evidently, excited is the one-way TIR mode, because the field amplitude does not peak at the Si-InSb interface. The simulated results for the case of $d = 14.4\ \mu$m are shown in Fig. 3(c). One TIR mode propagating backward is excited on the left side of the source, while two TIR modes propagating forward are excited on its right side, where clear interference pattern is generated. To examine the robustness of one-way TIR mode, we performed a further simulation for the case of $d = 6.8\ \mu$m but with an obstacle at 160 μm away from the source. The obstacle is a metal rod with the radius $r_o = 4\ \mu$m, and its center lies at the Si-InSb interface. Figure 3(b) shows that when excited waves reach the obstacle, they go around it and then continue to travel forward. The field amplitudes before and behind the obstacle are identical, so the one-way TIR mode is immune to backscattering. In all above simulations, the metal is set to be PEC. We also performed simulations for the realistic cases where the metal is Cu instead of PEC. The obtained field patterns are almost identical to those in Figs. 3(a)-3(c). However, in the case with the obstacle, our numerical analysis shows that the modal power behind the Cu rod is reduced by nearly 9%, and the energy dissipation is mainly caused by the Cu rod due to the enhanced local field around it. Anyway, all simulated results agree well with the predicted dispersion properties of the system.

We further investigate the one-way TIR mode in the premise of broad COWP bandwidth (which requires that $d \leq d_c$). In Fig. 2(a), it is seen that the propagation constant (k) of the

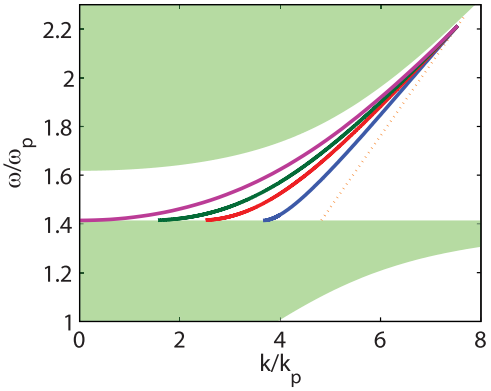

Fig. 4. (Color online) Dispersion curves of one-way TIR mode for different d values. From right to left: $d = 0.045\lambda_p$, $0.02\lambda_p$, $0.01\lambda_p$, and 0. The other parameters are the same as in Fig. 1.

one-way TIR mode is always positive in the case of $d = d_c$. For the one-way TIR mode, the minimal value (k_{min}) of k occurs at $\omega = \omega_{r,b}$. As $\omega \to \omega_{r,b}$, $\varepsilon_1 \to 0$ and $\varepsilon_v \to \infty$, from Eq. (3) we thus have

$$k_{min} = \frac{\varepsilon_2}{\varepsilon_r} p \tan(pd), \tag{5}$$

where $\varepsilon_2 = \varepsilon_\infty(\omega_c/\omega_{r,b}) > 0$, and $p = \sqrt{\varepsilon_r k_0^2 - k_{min}^2}$ with $k_0 = \omega_{r,b}/c$. Clearly, the value of k_{min} is always positive for any d (below d_c), i.e., the COWP band always lies in the positive-k region. Furthermore, it is clear from Eq. (5) that k_{min} decreases when d decreases (if when d decreases k_{min} increases, then p would decreases and so would $p\tan(pd)$, and consequently, the two sides of the equation would be unequal), and $k_{min} \to 0$ as $d \to 0$. To show this, the dispersion bands of one-way TIR mode for the different thicknesses $d = 0.045\lambda_p$, $0.02\lambda_p$, $0.01\lambda_p$, and 0 are displayed in Fig. 4. In the limit of $d = 0$, the system reduces to a bilayer structure, and the one-way mode becomes a surface wave, whose dispersion relation reduces to $k = \sqrt{\varepsilon_1}k_0$, where $\varepsilon_1 = 0$ at $\omega = \omega_{r,b}$. Note that in this case the light cone of Si also vanishes in physics.

It is interesting if the one-way TIR mode could more effectively match with the fundamental mode of conventional optical waveguide than one-way SMPs. To clarify this, we simulated wave transmission in a coupling system [see Fig. 5(e)], in which a uniform InSb-Si-metal structure (first section) is linked with a uniform optical waveguide (third section) through a tapered structure (second section) with the length $L_t = 390\ \mu$m. The first section has the same parameters as those in Fig. 2(a). In the second section, the boundaries of InSb and metal gradually depart from the Si layer, and the empty spaces are filled with crystal quartz (CQ) of the relative permittivity $\varepsilon_{cq} = 5.3$ [16]. As the thickness d_c is too thin for the core layer of optical waveguide, the Si layer is also gradually widened in the second section. The optical waveguide is formed by a Si layer of the thickness $D = 18\ \mu$m surrounded by CQ. This optical waveguide supports single-mode (TM_0) propagation when $f < 3.3$ THz. In what follows, for convenience, the interface between the first and second

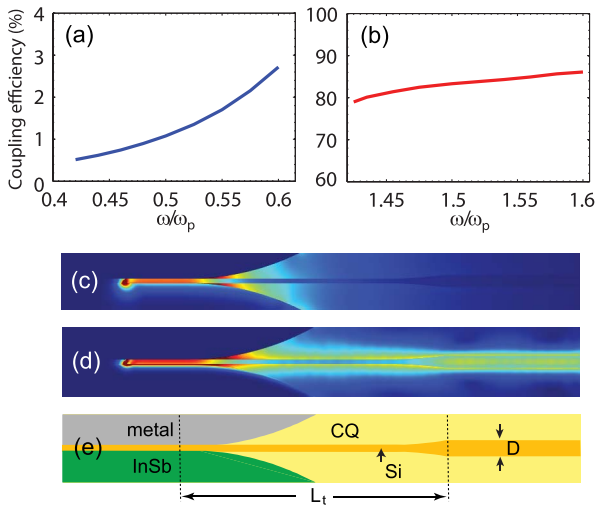

Fig. 5. (Color online) (a), (b) Coupling efficiency versus frequency. (c) Simulated electric field amplitudes for $\omega = 0.5\omega_p$. (d) Simulated electric field amplitudes for $\omega = 1.5\omega_p$. (e) Schematic of the coupling system. The parameters of the InSb-Si-metal structure are the same as in Fig. 2(a). The other parameters are $D = 18$ μm, $L_t = 390$ μm, and $\varepsilon_{cq} = 5.3$.

sections, and the one between the second and third sections are referred to as interfaces 1 and 2, respectively.

Figures 5(a) and 5(b) show the coupling efficiency from the InSb-Si-metal waveguide to the conventional optical waveguide. In the frequency range $[0.4074\omega_p, 0.6180\omega_p]$, which corresponds to the COWP band for one-way SMPs, the coupling efficiency is below 3%. However, in the frequency range $[1.414\omega_p, 1.618\omega_p]$, which corresponds to the COWP band for the one-way TIR mode, the coupling efficiency is almost larger than 80% over the whole range. To illustrate vividly the two different coupling behaviors, Figs. 5(c) and 5(d) display the simulated electric field amplitudes at the frequencies $\omega = 0.5\omega_p$ (i.e.,$f = 1$ THz) and $1.5\omega_p$ (i.e.,3 THz), respectively. When $\omega = 0.5\omega_p$, one-way SMP is excited in the first section of the system. Note that for this case the external magnetic field is reversed to make SMP propagating forward. As seen in Fig. 5(c), when SMP propagating forward reaches interface 1, it totally transmits into the second section, and meanwhile it is almost divided into two parts, one part is coupled into radiation waves, which are finally absorbed by the perfectly matched layer [17] around the computation domain, and the other part is coupled into SMP sustained by the interface of InSb and CQ. Consequently, almost no guiding wave is observed in the optical waveguide. When $\omega = 1.5\omega_p$, one-way TIR mode is excited in the first section, and when the excited wave reaches interface 1, it totally transmits into the second section as well. Evidently, the wave in the second section is confined to the Si layer. When the wave further reaches interface 2, it naturally transmits into the optical waveguide. So it is true that one-way waveguide based on the TIR mode can more effectively match with conventional optical waveguide than based on SMPs.

III. Conclusion

In conclusion, we have shown that in the semiconductor-dielectric-metal structure there exists one-way mode which is guided by the TIR mechanism. The dispersion band of the one-way mode is located within the upper semiconductor bandgap. This one-way TIR mode can be immune to backscattering, and the related COWP bandwidth equals to the whole semiconductor bandgap when the guiding-layer thickness is smaller than a certain value. By numerical simulation, it has been shown that compared to one-way SMPs, the one-way TIR mode can more effectively match with the fundamental mode of conventional optical waveguide. We expect these results to enable a new class of nonreciprocal optical devices which are well compatible with existing optical technology.

References

[1] F. D. M. Haldane and S. Raghu, "Possible realization of directional optical waveguides in photonic crystals with broken time-reversal symmetry," *Phys. Rev. Lett.*, vol. 100, no. 1, pp. 013904-1–013904-4, Jan. 2008.

[2] S. Raghu and F. D. M. Haldane, "Analogs of quantum-Hall-effect edge states in photonic crystals," *Phys. Rev. A, Gen. Phys.*, vol. 78, no. 3, pp. 033834-1–033834-21, Sep. 2008.

[3] Z. Wang, Y. D. Chong, J. D. Joannopoulos, and M. Soljačić, "Reflection-free one-way edge modes in a gyromagnetic photonic crystal," *Phys. Rev. Lett.*, vol. 100, p. 013905, Jan. 2008.

[4] Z. Wang, Y. Chong, J. D. Joannopoulos, and M. Soljačić, "Observation of unidirectional backscattering-immune topological electromagnetic states," *Nature*, vol. 461, pp. 772–775, Oct. 2009.

[5] X. Ao, Z. Lin, and C. T. Chan, "One-way edge mode in a magneto-optical honeycomb photonic crystal," *Phys. Rev. B, Condens. Matter*, vol. 80, no. 3, pp. 033105-1–033105-4, Jul. 2009.

[6] J. J. Brion, R. F. Wallis, A. Hartstein, and E. Burstein, "Theory of surface magnetoplasmons in semiconductors," *Phys. Rev. Lett.*, vol. 28, no. 22, pp. 1455–1458, May 1972.

[7] Z. Yu, G. Veronis, Z. Wang, and S. Fan, "One-way electromagnetic waveguide formed at the interface between a plasmonic metal under a static magnetic field and a photonic crystal," *Phys. Rev. Lett.*, vol. 100, no. 2, pp. 023902-1–023902-4, Jan. 2008.

[8] V. Kuzmiak, S. Eyderman, and M. Vanwolleghem, "Controlling surface plasmon polaritons by a static and/or time-dependent external magnetic field," *Phys. Rev. B, Condens. Matter*, vol. 86, no. 4, pp. 045403-1–045403-9, Jul. 2012.

[9] B. Hu, Q. J. Wang, and Y. Zhang, "Broadly tunable one-way terahertz plasmonic waveguide based on nonreciprocal surface magneto plasmons," *Opt. Lett.*, vol. 37, no. 11, pp. 1895–1897, Jun. 2012.

[10] L. F. Shen, Y. You, Z. Wang, and X. Deng, "Backscattering-immune one-way surface magnetoplasmons at terahertz frequencies," *Opt. Exp.*, vol. 23, no. 2, pp. 950–962, Jan. 2015.

[11] X. Zhang, W. Li, and X. Jiang, "Confined one-way mode at magnetic domain wall for broadband high-efficiency one-way waveguide, splitter and bender," *Appl. Phys. Lett.*, vol. 100, no. 4, pp. 041108-1–041108-4, Jan. 2012.

[12] X. Deng, L. Hong, X. Zheng, and L. Shen, "One-way regular electromagnetic mode immune to backscattering," *Appl. Opt.*, vol. 54, no. 14, pp. 4608–4612, May 2015.

[13] A. W. Snyder and J. D. Love, *Optical Waveguide Theory*, London, U.K.: Chapman & Hall, 1983.

[14] J. G. Rivas, C. Janke, P. H. Bolivar, and H. Kurz, "Transmission of THz radiation through InSb gratings of subwavelength apertures," *Opt. Exp.*, vol. 13, no. 3, pp. 847–859, Feb. 2015.

[15] M. A. Ordal, R. J. Bell, R. W. Alexander, L. L. Long, and M. R. Querry, "Optical properties of fourteen metals in the infrared and far infrared: Al, Co, Cu, Au, Fe, Pb, Mo, Ni, Pd, Pt, Ag, Ti, V, and W," *Appl. Opt.*, vol. 24, no. 24, pp. 4493–4499, Dec. 1985.

[16] V. Sanphuang, W. G. Yeo, J. L. Volakis, and N. K. Nahar, "THz transparent metamaterials for enhanced spectroscopic and imaging measurements," *IEEE Trans. THz Sci. Technol.*, vol. 5, no. 1, pp. 117–123, Jan. 2015.

[17] A. Taflove and S. C. Hagness, *Computational Electrodynamics: The Finite-Difference Time-Domain Method*. Boston, MA, USA: Artech House, 2000.